

Conditions for the Invar effect in $\text{Fe}_{1-x}\text{A}_x$ ($A = \text{Pt}, \text{Ni}$)

François Liot^{1,2,3‡}

¹ Norinvar, 59 la rue, 50110 Bretteville, France

² Department of Computational Materials Design (CM), Max-Planck-Institut für Eisenforschung GmbH, D-40237 Düsseldorf, Germany

³ Department of Physics, Chemistry, and Biology (IFM), Linköping University, SE-581 83 Linköping, Sweden

E-mail: f.liot@norinvar.com

Abstract. We present a necessary condition under which a collinear ferromagnet $\text{Fe}_{1-x}\text{A}_x$ ($A = \text{Pt}, \text{Ni}$) with disordered face-centered-cubic structure exhibits the Invar effect. The condition involves the rate at which the fraction of Fe moments that are antiferromagnetically aligned with the magnetization fluctuates as the system is heated, $dx^{\text{Fe}\downarrow}/dT$. Another contributing factor is the magnetostructural coupling $\kappa = -(1/V)(\partial V/\partial x^{\text{Fe}\downarrow})_T$, where the volume $V(T, x^{\text{Fe}\downarrow})$ corresponds to a homogeneous ferromagnetic state, a partially disordered local moment state, or a disordered local moment state depending on the value of $x^{\text{Fe}\downarrow}$. According to the criterion, the Invar phenomenon occurs only when the thermal expansion arising from the temperature dependence of the fraction of Fe moments which point down $-1/3 \kappa dx^{\text{Fe}\downarrow}/dT$ compensates for the thermal expansion associated with the anharmonicity of lattice vibrations in a wide temperature interval. Upon further investigation, we provide evidence that only alloys with strong magnetostructural coupling at zero Kelvin can show the Invar effect.

PACS numbers: 65.40.De, 71.15.Mb, 75.10.Hk, 75.50.Bb

‡ Present address: Norinvar, 59 la rue, 50110 Bretteville, France.

1. Introduction

Disordered face-centered-cubic (fcc) $\text{Fe}_{0.72}\text{Pt}_{0.28}$ and $\text{Fe}_{0.65}\text{Ni}_{0.35}$ alloys have remained at the forefront of condensed matter theory for more than sixty years, owing to their rich variety of intriguing physical properties. Their linear thermal expansion coefficient (LTEC), α , is anomalously small [$\alpha(T) \ll 10^{-5} \text{ K}^{-1}$] over a wide range of temperature [1, 2], a phenomenon known as the Invar effect. Their spontaneous volume magnetostriction, w_s , measured at $T = 0 \text{ K}$ greatly exceeds that in body-centered-cubic (bcc) Fe and fcc Ni [3]. Their reduced magnetostriction, $w_s/w_s(0)$, scales with the square of the reduced magnetization, $[M/M(0)]^2$, up to a temperature near the Curie temperature, T_C [3, 4, 5, 6]. Surprisingly, only one of these two ferromagnets, namely $\text{Fe}_{0.65}\text{Ni}_{0.35}$, shows a peculiar thermal dependence of the reduced magnetization [4, 5].

Understanding all of the abovementioned phenomena within one framework is still a major open challenge. The most common theoretical explanation for the Invar effect involves the so-called 2γ -state model, where the iron atoms can switch between two magnetic states with different atomic volumes as the temperature is raised [7]. This theory, however, seems incompatible with the results of Mössbauer [8] and neutron experiments [9]. Another popular explanation emphasizes the importance of non-collinearity of the local magnetic moments on iron sites [10, 11], though experiments undertaken to detect such non-collinearity have not found it [12]. An alternative scenario with a purely magnetic origin for the Invar effect has been proposed [13]: the phenomenon is caused by anomalous thermal evolution of the magnitude of Fe moments. It is supported by a recent work on iron-platinum alloys [14] which involves *ab initio* density functional theory (DFT) calculations and the disordered local moment (DLM) model [15, 16]. However, the method employed in [14] cannot be extended to iron-nickel alloys. Thus, it is unable to provide a unified picture for the Invar effect in $\text{Fe}_{0.72}\text{Pt}_{0.28}$ and $\text{Fe}_{0.65}\text{Ni}_{0.35}$ and another treatment is called for.

A theoretical framework [17] has recently been designed to address the spontaneous magnetization, the spontaneous volume magnetostriction, and their relationship in $\text{Fe}_{0.72}\text{Pt}_{0.28}$ and $\text{Fe}_{0.65}\text{Ni}_{0.35}$ in the temperature interval $0 \leq T/T_C < 1$. Taking a similar approach as in [14] and [18], alloys in equilibrium at temperature T have been modelled by random substitutional alloys in homogeneous ferromagnetic (FM) states, partially disordered local moment (PDLM) states, or DLM states depending on the fraction of Fe moments which are antiferromagnetically aligned with the magnetization at T , $x^{\text{Fe}\downarrow}(T)$. The procedure could be divided into the following three stages. In the first stage, physical properties of interest (volume and magnetization) have been calculated for FM ($x^{\text{Fe}\downarrow} = 0$), PDLM ($0 < x^{\text{Fe}\downarrow} < 1/2$), and DLM ($x^{\text{Fe}\downarrow} = 1/2$) states using *ab initio* DFT. In the second stage, the thermal evolution of the fraction of Fe moments which point down has been determined by noticing that an accurate description of the reduced magnetization is provided by a function of this form

$$\frac{M(T)}{M(0)} = \left[1 - s \left(\frac{T}{T_C} \right)^{3/2} - (1 - s) \left(\frac{T}{T_C} \right)^p \right]^q \quad (1)$$

Table 1. The volume $V(0)$, the bulk modulus $B(0)$, and the Grüneisen constant $\gamma(0)$ for $\text{Fe}_{0.72}\text{Pt}_{0.28}$, $\text{Fe}_{0.65}\text{Ni}_{0.35}$, and $\text{Fe}_{0.2}\text{Ni}_{0.8}$, according to EMT0 calculations. All of these quantities are calculated for homogeneous ferromagnetic states.

	volume (\AA^3)	bulk modulus (GPa)	Grüneisen constant
$\text{Fe}_{0.72}\text{Pt}_{0.28}$	13.44	177	2
$\text{Fe}_{0.65}\text{Ni}_{0.35}$	11.59	177	2
$\text{Fe}_{0.2}\text{Ni}_{0.8}$	11.13	193	2

and assuming that $x^{\text{Fe}\downarrow}$ obeys the following equation

$$x^{\text{Fe}\downarrow}(T) = \frac{1}{2} - \left[\frac{1}{2} - x^{\text{Fe}\downarrow}(0) \right] \left[1 - \left(\frac{T}{T_C} \right)^p \right]^q. \quad (2)$$

In the third and final step, the outputs from the previous steps have been combined to explore how the magnetization and the magnetostriction vary as the system is heated. Direct comparison between simulations results and experimental measurements has provided validation for the approach. The study supports the following ideas. The alloys at $T = 0$ K share several physical properties: the magnetization in a PDLM state collapses as the fraction of Fe moments which point down increases, following closely

$$M(0) - 2M(0)x^{\text{Fe}\downarrow}, \quad (3)$$

while the volume shrinks, following closely

$$V(0) - 4[V(0) - V(1/2)]x^{\text{Fe}\downarrow}(1 - x^{\text{Fe}\downarrow}); \quad (4)$$

the volume in the FM state greatly exceeds that in the DLM state; $x^{\text{Fe}\downarrow}(0)$ is close to 0. These common properties can account for a variety of intriguing phenomena displayed by both alloys, including the anomaly in the magnetostriction at $T = 0$ K and, more surprisingly perhaps, the scaling between the reduced magnetostriction and the reduced magnetization squared below the Curie temperature. However, the thermal evolution of the fraction of Fe moments which point down depends strongly on the alloy under consideration. This, in turn, can explain the observed marked difference in the temperature dependence of the reduced magnetization between the two alloys.

This paper deals with the Invar effect in collinear ferromagnets $\text{Fe}_{1-x}\text{A}_x$ ($A = \text{Pt, Ni}$) with disordered fcc structure. The rich variety of thermal expansion displayed by these materials has firmly been established by experiments [6, 19]. This makes them particularly attractive for testing our general approach, identifying conditions under which an alloy shows the Invar effect, and investigating the mechanism of the Invar phenomenon. In principle, the LTEC can be derived from the configuration-averaged free energy which depends explicitly on volume and temperature. In practice, application of DFT to *ab initio* calculations of a finite-temperature average free energy remains difficult, even in the adiabatic approximation where the electronic, the vibrational, and the magnetic contributions are treated separately. One of the major issues in implementing this strategy is how to incorporate magnetism correctly within the current approximations to the exchange and correlation functional [20]. Our simulation technique can be viewed as an extension of [17] in which the vibrational

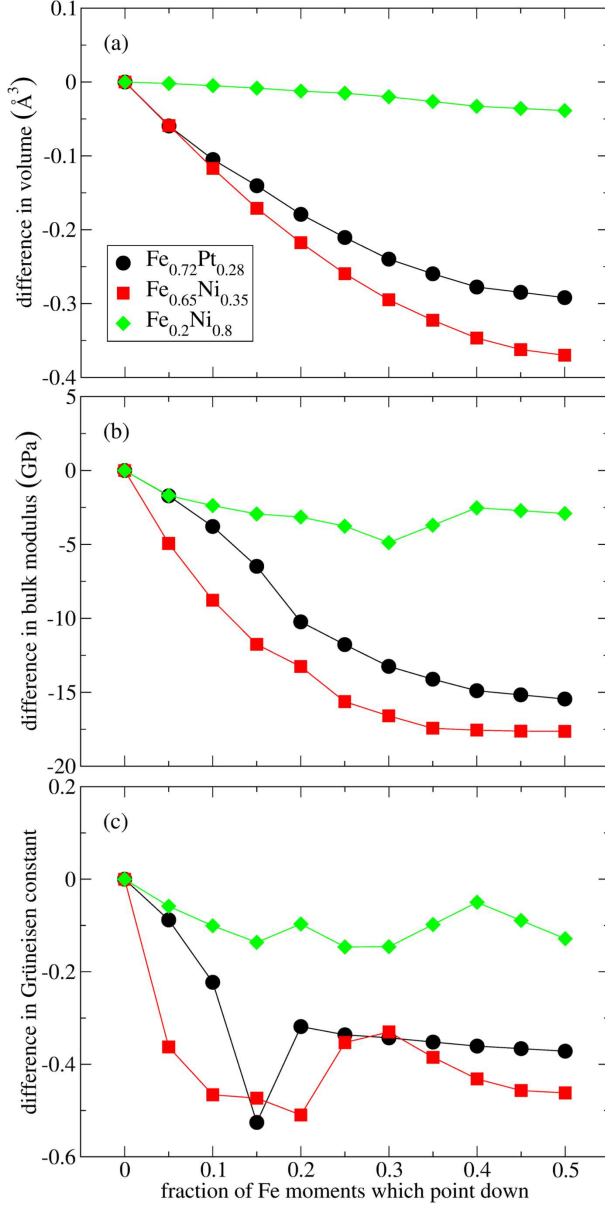


Figure 1. The difference in volume $[V(x^{\text{Fe}\downarrow}) - V(0)]$ [panel (a)], the difference in bulk modulus $[B(x^{\text{Fe}\downarrow}) - B(0)]$ [panel (b)], and the difference in Grüneisen constant $[\gamma(x^{\text{Fe}\downarrow}) - \gamma(0)]$ [panel (c)] plotted against the fraction of Fe moments which point down for $\text{Fe}_{0.72}\text{Pt}_{0.28}$, $\text{Fe}_{0.65}\text{Ni}_{0.35}$, and $\text{Fe}_{0.2}\text{Ni}_{0.8}$. Symbols show results of EMTO calculations. Note that the values for $V(0)$, $B(0)$, and $\gamma(0)$ are displayed in table 1.

contribution to the average free energy is treated within the Debye-Grüneisen model [21, 22, 23, 24]. Section 2 is devoted to computational details. Section 3 presents a comprehensive discussion of our results. As we shall see, this work challenges the conventional picture of the Invar effect as resulting from peculiar magnetic behaviour [10, 11, 13, 14, 25].

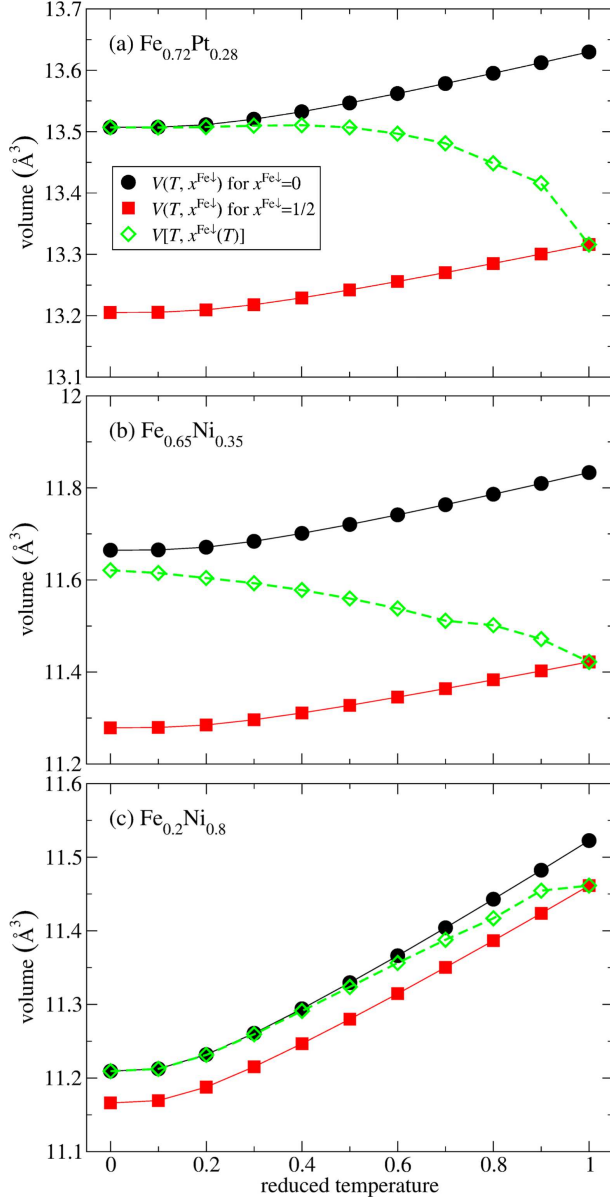


Figure 2. The volumes $V(T, 0)$, $V(T, 1/2)$, and $V[T, x^{\text{Fe}\downarrow}(T)]$ plotted against the reduced temperature T/T_C for $\text{Fe}_{0.72}\text{Pt}_{0.28}$ [panel (a)], $\text{Fe}_{0.65}\text{Ni}_{0.35}$ [panel (b)], and $\text{Fe}_{0.2}\text{Ni}_{0.8}$ [panel (c)].

2. Computational methods

To address the Invar effect in collinear ferromagnets $\text{Fe}_{1-x}\text{A}_x$ ($A = \text{Pt}, \text{Ni}$) with disordered fcc structure, we extend the scheme developed in [17] to include atomic vibrations. $\text{Fe}_{1-x}\text{A}_x$ alloys in equilibrium at temperature T in the range $0 \leq T/T_C < 1$ are modelled by random substitutional alloys in FM, PDLM, or DLM states depending on $x^{\text{Fe}\downarrow}(T)$. The method remains divided into three main stages.

As a first step, we perform calculations of the volume $V(T, x^{\text{Fe}\downarrow})$ for various temperatures and FM ($x^{\text{Fe}\downarrow} = 0$), PDLM ($0 < x^{\text{Fe}\downarrow} < 1/2$), and DLM ($x^{\text{Fe}\downarrow} = 1/2$)

states. For a fixed value of T and $x^{\text{Fe}\downarrow}$, the computational process is as follows:

- (i) We calculate the total energy $E(r, x^{\text{Fe}\downarrow})$ for various Wigner-Seitz radii. This is done within the framework of the exact muffin-tin orbitals (EMTO) theory in combination with the full charge density (FCD) technique [26]. Further details can be found in [17].
- (ii) We deduce from the results of step (i) the Wigner-Seitz radius $r(x^{\text{Fe}\downarrow})$, the volume $V(x^{\text{Fe}\downarrow})$, the bulk modulus $B(x^{\text{Fe}\downarrow})$, and the Grüneisen constant $\gamma(x^{\text{Fe}\downarrow})$ [21].
- (iii) For each Wigner-Seitz radius chosen in step (i), we estimate the contribution to the Helmholtz free energy $F_{\text{vib}}(T, r, x^{\text{Fe}\downarrow})$ from the outputs of step (ii)

$$F_{\text{vib}}(T, r, x^{\text{Fe}\downarrow}) = E_{\text{D}}(T, r, x^{\text{Fe}\downarrow}) - TS_{\text{D}}(T, r, x^{\text{Fe}\downarrow}), \quad (5)$$

where the vibrational energy and the vibrational entropy take the simple form

$$E_{\text{D}}(T, r, x^{\text{Fe}\downarrow}) = \frac{9}{8}k_{\text{B}}\Theta(r, x^{\text{Fe}\downarrow}) + 3k_{\text{B}}TD[\Theta(r, x^{\text{Fe}\downarrow})/T] \quad (6)$$

and

$$S_{\text{D}}(T, r, x^{\text{Fe}\downarrow}) = 4k_{\text{B}}D[\Theta(r, x^{\text{Fe}\downarrow})/T] - 3k_{\text{B}}\ln[1 - e^{-\Theta(r, x^{\text{Fe}\downarrow})/T}]. \quad (7)$$

Here, D denotes the Debye function. In analogy with [21, 23], we choose the Debye temperature $\Theta(r, x^{\text{Fe}\downarrow})$ to be given by

$$\Theta(r, x^{\text{Fe}\downarrow}) = \Theta_0(x^{\text{Fe}\downarrow}) \left[\frac{r(x^{\text{Fe}\downarrow})}{r} \right]^{3\gamma(x^{\text{Fe}\downarrow})}, \quad (8)$$

where $\Theta_0(x^{\text{Fe}\downarrow})$ scales with $[r(x^{\text{Fe}\downarrow})B(x^{\text{Fe}\downarrow})/M]^{1/2}$. We take the proportionality factor from [23].

- (iv) We minimize the sum $E + F_{\text{vib}}$ with respect to r to obtain the volume $V(T, x^{\text{Fe}\downarrow})$.

As a second step, we investigate how heating the alloy affects its fraction of Fe moments which point down. The adopted method has already been described elsewhere [17].

In the third and final step, we combine the outputs from the two previous stages to explore how the volume $V[T, x^{\text{Fe}\downarrow}(T)]$ and the anomalous contribution to the LTEC $\alpha_{\text{a}}(T)$ vary as the temperature is raised. To allow for direct comparison between simulations and experiments [27], we conveniently define $\alpha_{\text{a}}(T)$ as the difference between $\alpha(T)$ and $\alpha_{\text{n}}(T)$, where the normal contribution to the LTEC measures the expansion that would occur if we heated the alloy in a DLM ('paramagnetic') state

$$\alpha_{\text{n}}(T) = \left[\frac{1}{3V} \left(\frac{\partial V}{\partial T} \right) \right]_{x^{\text{Fe}\downarrow}} (T, 1/2). \quad (9)$$

It is instructive to reexpress $\alpha_{\text{a}}(T)$ as the sum of two terms

$$\alpha_{\text{a},1}(T) = \left[\frac{1}{3V} \left(\frac{\partial V}{\partial T} \right) \right]_{x^{\text{Fe}\downarrow}} [T, x^{\text{Fe}\downarrow}(T)] - \left[\frac{1}{3V} \left(\frac{\partial V}{\partial T} \right) \right]_{x^{\text{Fe}\downarrow}} (T, 1/2) \quad (10)$$

and

$$\alpha_{\text{a},2}(T) = \left[\frac{1}{3V} \left(\frac{\partial V}{\partial x^{\text{Fe}\downarrow}} \right) \right]_T [T, x^{\text{Fe}\downarrow}(T)] \frac{dx^{\text{Fe}\downarrow}}{dT}(T) \quad (11)$$

that corresponds to two distinct sources of anomaly: one associated with the expansion that would occur if we heated the alloy *without changing the configuration of Fe moments* and another one linked with the expansion that would occur if we changed the configuration of Fe moments, *but did not otherwise heat the system*. This latter contribution to $\alpha_a(T)$ can be conveniently written as the product of the prefactor $-1/3$, the magnetostructural coupling

$$\kappa[T, x^{\text{Fe}\downarrow}(T)] = \left[-\frac{1}{V} \left(\frac{\partial V}{\partial x^{\text{Fe}\downarrow}} \right)_T \right] [T, x^{\text{Fe}\downarrow}(T)], \quad (12)$$

and the rate at which the fraction of Fe moments which point down fluctuates as the system is heated $dx^{\text{Fe}\downarrow}/dT(T)$.

3. Results and discussion

According to experiments [6, 19], $\text{Fe}_{0.72}\text{Pt}_{0.28}$, $\text{Fe}_{0.65}\text{Ni}_{0.35}$, and $\text{Fe}_{0.2}\text{Ni}_{0.8}$ exhibit a wide variety of thermal behaviour, the Fe-rich alloys showing the Invar effect and the Fe-poor alloy presenting thermal expansion similar to that of a paramagnetic compound. For this reason, they represent a suitable choice for testing the predictive power of the method developed in section 2, formulating conditions for the occurrence of the Invar effect, and investigating the mechanism of the phenomenon.

3.1. Testing our approach

Table 1 shows the calculated volumes $V(0)$, bulk moduli $B(0)$, and Grüneisen constants $\gamma(0)$. Figure 1 displays the calculated differences in volumes $[V(x^{\text{Fe}\downarrow}) - V(0)]$, bulk moduli $[B(x^{\text{Fe}\downarrow}) - B(0)]$, and Grüneisen constants $[\gamma(x^{\text{Fe}\downarrow}) - \gamma(0)]$ for FM, PDL, and DLM states. Note that the structural data have already been discussed [17]. Regardless of the chemical nature of the alloy, the volume V shrinks with increasing the fraction of Fe moments which point down, following closely (4). The volume for the FM state and the volume for the DLM state differ by more than 0.25 \AA^3 in the Fe-rich alloys. The volume difference drops to 0.04 \AA^3 when switching to the Fe-poor alloy. We now turn to describe the materials' response to uniform compression. Whether we consider $\text{Fe}_{0.72}\text{Pt}_{0.28}$, $\text{Fe}_{0.65}\text{Ni}_{0.35}$, or $\text{Fe}_{0.2}\text{Ni}_{0.8}$, the bulk modulus for the FM state lies within 175 and 195 GPa. This is consistent with measurements performed on $\text{Fe}_{0.72}\text{Pt}_{0.28}$ and Ni [28]. The effect of raising $x^{\text{Fe}\downarrow}$ on the bulk modulus B mirrors to a certain extent that seen in panel (a) for the volume V : (i) The bulk modulus decreases in the Invar alloys, revealing that these materials become easier to squeeze. (ii) The difference $[B(0) - B(1/2)]$, which amounts to 15 in $\text{Fe}_{0.72}\text{Pt}_{0.28}$, 18 in $\text{Fe}_{0.65}\text{Ni}_{0.35}$, and 3 GPa in $\text{Fe}_{0.2}\text{Ni}_{0.8}$, is considerably larger in the Fe-rich alloys. We note in passing that these findings might shed light on anomalies observed in measurements of bulk moduli [11, 28, 29, 30]. While we discuss figure 1, we point out that numerical noise poses a significant problem for the determination of the Grüneisen constants.

Figure 2 illustrates how the volumes $V(T, 0)$, $V(T, 1/2)$, and $V[T, x^{\text{Fe}\downarrow}(T)]$ change with varying the temperature in the range $0 \leq T/T_C < 1$. A useful way to analyze these

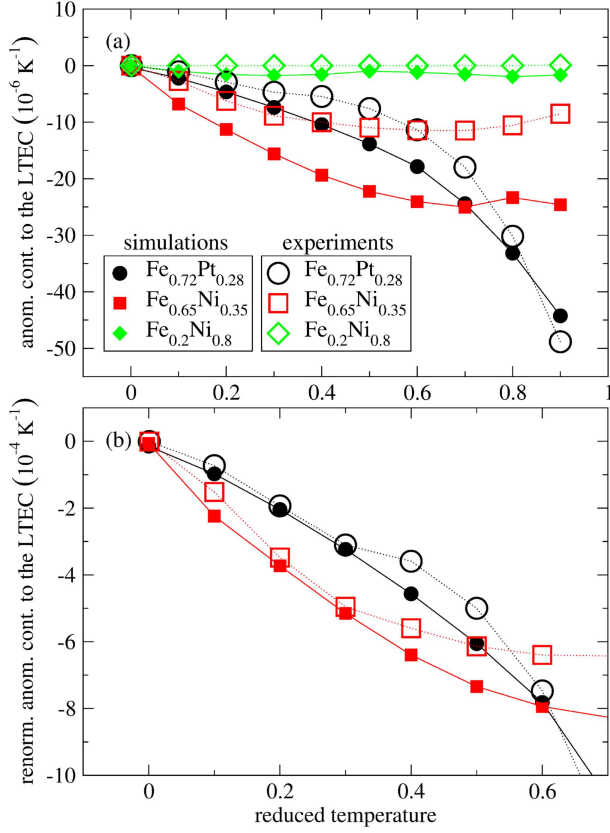


Figure 3. Panel (a): The anomalous contribution to the LTEC evaluated at temperature T plotted against the reduced temperature for $\text{Fe}_{0.72}\text{Pt}_{0.28}$, $\text{Fe}_{0.65}\text{Ni}_{0.35}$, and $\text{Fe}_{0.2}\text{Ni}_{0.8}$. Panel (b): The renormalized anomalous contribution for the two Fe-rich alloys. Filled symbols show results of numerical calculations. Open symbols display experimental data [6, 19, 31, 32].

data is as follows. Imagine that the magnetic configuration were fixed ($dx^{\text{Fe}\downarrow}/dT = 0$). Let us call the corresponding curve $V[T, x^{\text{Fe}\downarrow}(0)]$; the curve for $\text{Fe}_{0.72}\text{Pt}_{0.28}$ and $\text{Fe}_{0.2}\text{Ni}_{0.8}$ is the uppermost black curve in panels (a) and (c). Then the material would not exhibit the Invar effect. This would also be the case if all of the curves $V(T, x^{\text{Fe}\downarrow})$ for $0 \leq x^{\text{Fe}\downarrow} \leq 1/2$ superimposed [$(\partial V/\partial x^{\text{Fe}\downarrow})_T = 0$]. In reality, however, raising the temperature from T_1 to T_2 causes the material to demagnetize, and the value of $x^{\text{Fe}\downarrow}$ changes accordingly. One may say that the system hops from the curve $V[T, x^{\text{Fe}\downarrow}(T_1)]$ to the curve $V[T, x^{\text{Fe}\downarrow}(T_2)]$, resulting in a volume given by the curve $V[T, x^{\text{Fe}\downarrow}(T)]$. This is shown as a dashed line. Insofar as panel (b) allows us to judge for $\text{Fe}_{0.65}\text{Ni}_{0.35}$, each hop is to a curve lower than the last, cancelling the upward trend of each individual curve: this is the essence of the Invar effect. In section 3.2, we present a necessary condition under which an alloy shows the Invar effect. Consistent with the analysis of figure 2, the criterion involves $\alpha_{a,2} = -1/3 \kappa dx^{\text{Fe}\downarrow}/dT$.

In panel (a) of figure 3, we plot the calculated anomalous contribution to the LTEC $\alpha_a(T)$ against the reduced temperature for $\text{Fe}_{0.72}\text{Pt}_{0.28}$, $\text{Fe}_{0.65}\text{Ni}_{0.35}$, and $\text{Fe}_{0.2}\text{Ni}_{0.8}$. Irrespective of the material under consideration, $\alpha_a(T)$ exhibits a negative sign opposite

to $\alpha_n(T)$. However, only the Fe-rich materials possess the exceptional property that $\alpha_a(T)$ compensates for $\alpha_n(T)$ in a wide temperature range. Thus the approach predicts the occurrence of the Invar effect in $\text{Fe}_{0.72}\text{Pt}_{0.28}$ and $\text{Fe}_{0.65}\text{Ni}_{0.35}$ and its absence in $\text{Fe}_{0.2}\text{Ni}_{0.8}$. This perfectly matches experimental findings [19, 31].

To further evaluate the predictive power of the method, we compare the calculated renormalized anomalous contribution to the LTEC $\tilde{\alpha}_a(T) = \alpha_a(T)/w_s(0)$ with experimental observations [6, 19, 31, 32] for the Invar alloys in panel (b) of figure 3. Note that we extract the calculated values for $w_s(0) = \{V[0, x^{\text{Fe}\downarrow}(0)] - V(0, 1/2)\}/V(0, 1/2)$ from figure 2 and obtain 2.29% for $\text{Fe}_{0.72}\text{Pt}_{0.28}$ and 3.03% for $\text{Fe}_{0.65}\text{Ni}_{0.35}$. Panel (b) of figure 3 reveals a good quantitative agreement between simulations and experiments. For instance, the curve for $\text{Fe}_{0.72}\text{Pt}_{0.28}$ intersects that for $\text{Fe}_{0.65}\text{Ni}_{0.35}$ at $T/T_C = 0.01$ and 0.6 according to simulations and $T/T_C = 0$ and 0.55 according to experiments. Another example involves the difference between $\tilde{\alpha}_a(T)$ of the former alloy and that of the latter estimated at $T/T_C = 0.3$: The calculated quantity is $1.91 \cdot 10^{-4} \text{ K}^{-1}$, while the corresponding measured value amounts to $1.85 \cdot 10^{-4} \text{ K}^{-1}$.

Figure 3 provides strong evidence that the approach presented in this paper captures the essential physics of the Invar effect. This opens exciting opportunities for identifying conditions under which an alloy shows the Invar effect and investigating the mechanism of the phenomenon, which, in principle, can now be understood within the same framework as other intriguing observations [17], including: (i) the anomalously large magnetostriction in $\text{Fe}_{0.72}\text{Pt}_{0.28}$ and $\text{Fe}_{0.65}\text{Ni}_{0.35}$ at $T = 0 \text{ K}$, (ii) the peculiar temperature dependence of the reduced magnetization in $\text{Fe}_{0.65}\text{Ni}_{0.35}$, and (iii) the scaling of the reduced magnetostriction with the square of the reduced magnetization in $\text{Fe}_{0.72}\text{Pt}_{0.28}$ and $\text{Fe}_{0.65}\text{Ni}_{0.35}$ below the Curie temperature.

3.2. Identifying conditions under which an alloy shows the Invar effect

The decomposition of the anomalous contribution to the LTEC $\alpha_a(T)$ into its two parts $\alpha_{a,1}(T)$ and $\alpha_{a,2}(T)$ is plotted against T/T_C in figure 4 for $\text{Fe}_{0.72}\text{Pt}_{0.28}$, $\text{Fe}_{0.65}\text{Ni}_{0.35}$, and $\text{Fe}_{0.2}\text{Ni}_{0.8}$. The two competing terms $[(1/3V)(\partial V/\partial T)_{x^{\text{Fe}\downarrow}}](T, 1/2)$ and $[(1/3V)(\partial V/\partial T)_{x^{\text{Fe}\downarrow}}][T, x^{\text{Fe}\downarrow}(T)]$ balance each other almost completely, resulting in a very small $|\alpha_{a,1}(T)|$ (i.e., $|\alpha_{a,1}(T)|$ of the order of 10^{-6} K^{-1} , or less). It is clear that any strong deviation from zero shown by the anomalous contribution to the LTEC arises from $\alpha_{a,2}(T) = -1/3 \kappa[T, x^{\text{Fe}\downarrow}(T)] dx^{\text{Fe}\downarrow}/dT(T)$. Features in the structural behaviour of the materials which have been observed experimentally (see figure 3), but have remained unexplained, can now be interpreted on the basis of the abovementioned insight and our theoretical results displayed in figure 4: (i) The drop in the anomalous contribution to the LTEC in $\text{Fe}_{1-x}\text{Ni}_x$ at $T/T_C = 1/2$ when the nickel concentration is reduced from 0.8 to 0.35 arises from the steep decrease of the product of the magnetostructural coupling $\kappa[T, x^{\text{Fe}\downarrow}(T)]$ and the magnetic term $dx^{\text{Fe}\downarrow}/dT(T)$. (ii) The fact that the anomalous contribution to the LTEC in $\text{Fe}_{0.72}\text{Pt}_{0.28}$ diminishes significantly as T/T_C is raised from 0.5 to 0.9, whereas that in $\text{Fe}_{0.65}\text{Ni}_{0.35}$ does not reflect the different behaviours of

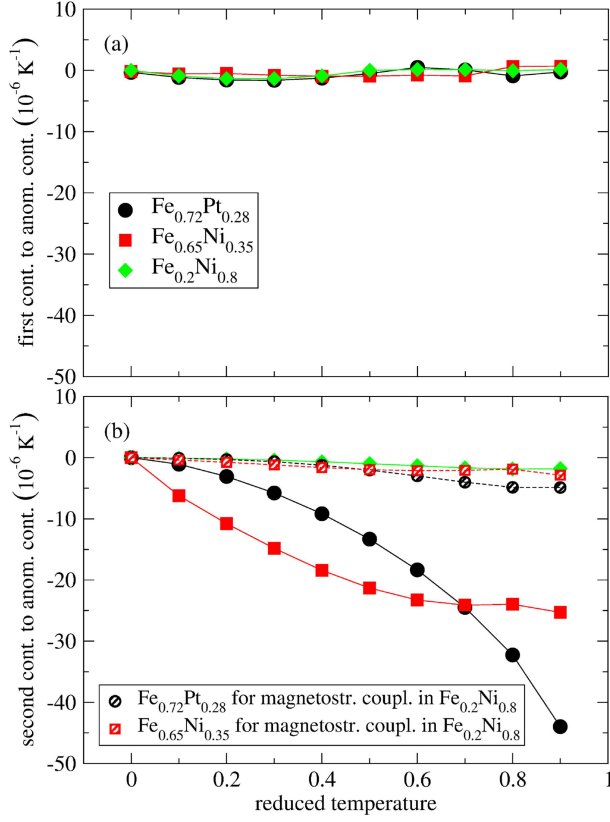


Figure 4. The two contributions $\alpha_{a,1}(T)$ [panel (a)] and $\alpha_{a,2}(T)$ [panel (b)] to $\alpha_a(T)$ plotted against the reduced temperature for $\text{Fe}_{0.72}\text{Pt}_{0.28}$, $\text{Fe}_{0.65}\text{Ni}_{0.35}$, and $\text{Fe}_{0.2}\text{Ni}_{0.8}$. Symbols show results of numerical calculations. Hatched symbols correspond to simulations performed for the two Fe-rich alloys with their magnetostructural coupling κ substituted by that of $\text{Fe}_{0.2}\text{Ni}_{0.8}$.

$\kappa dx^{\text{Fe}\downarrow}/dT$ in this interval: this physical quantity decreases drastically in the Fe-Pt case, but remains almost constant in that of Fe-Ni.

On the basis of figures 3 and 4, we argue that *the Invar phenomenon occurs only when the thermal expansion arising from the temperature dependence of the fraction of Fe moments which point down $\alpha_{a,2}$ compensates for the thermal expansion associated with the anharmonicity of lattice vibrations α_n in a wide temperature interval.*

A natural question to ask is: Why do some alloys fulfill this necessary condition for the occurrence of the Invar effect and others do not? To shed light on this matter, consider our results presented in figures 4 and 5. In $\text{Fe}_{0.2}\text{Ni}_{0.8}$, the magnetostructural coupling is weak at $T = 0 \text{ K}$ ($\kappa[0, x^{\text{Fe}\downarrow}(0)] = 0.74 \cdot 10^{-2}$) and $\alpha_{a,2}$ fails to counterbalance α_n over a broad temperature range. In the Fe-rich alloys, however, the magnetostructural coupling is especially strong ($\kappa[0, x^{\text{Fe}\downarrow}(0)] > 9 \cdot 10^{-2}$) and $\alpha_{a,2}$ compensates for α_n in a wide temperature interval. Interestingly, if we substitute their magnetostructural coupling κ by that of $\text{Fe}_{0.2}\text{Ni}_{0.8}$, the physical situation changes drastically, resembling that in $\text{Fe}_{0.2}\text{Ni}_{0.8}$. This supports the idea that only alloys with strong magnetostructural coupling at $T = 0 \text{ K}$ can show the Invar effect.

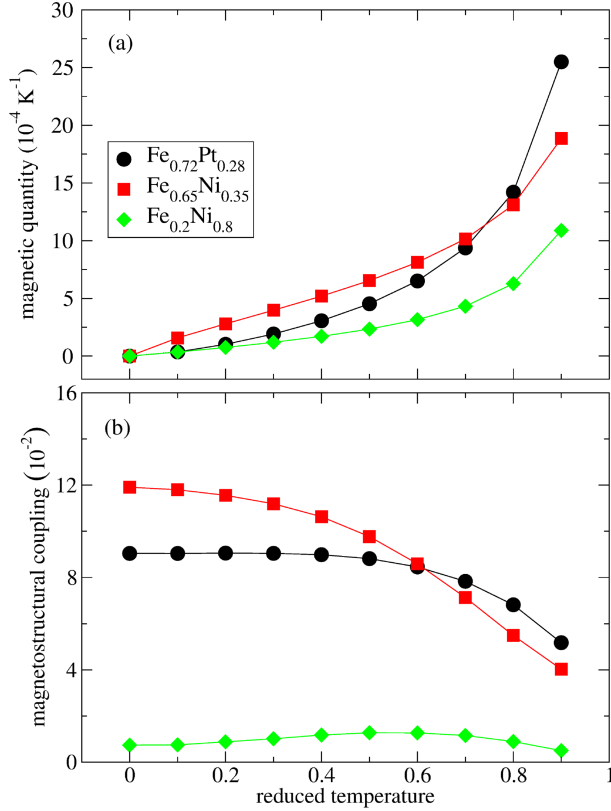


Figure 5. The magnetic quantity $dx^{\text{Fe}\downarrow}/dT(T)$ [panel (a)] and the magnetostructural coupling $\kappa[T, x^{\text{Fe}\downarrow}(T)]$ [panel (b)] plotted against the reduced temperature for Fe_{0.72}Pt_{0.28}, Fe_{0.65}Ni_{0.35}, and Fe_{0.2}Ni_{0.8}.

4. Conclusion

To address the Invar effect in collinear ferromagnets Fe_{1-x}A_x ($A = \text{Pt}, \text{Ni}$) with disordered fcc structure, we have extended the scheme developed in [17] to include atomic vibrations. Fe_{1-x}A_x alloys in equilibrium at temperature T in the range $0 \leq T/T_C < 1$ have been modelled by random substitutional alloys in FM, PDLM, or DLM states depending on $x^{\text{Fe}\downarrow}(T)$. The method has been divided into three main stages. As a first step, we have performed calculations of the volume $V(T, x^{\text{Fe}\downarrow})$ for various temperatures and FM, PDLM, and DLM states. As a second step, we have investigated how heating the alloy affects its fraction of Fe moments which point down. In the third and final step, we have combined the outputs from the two previous stages to explore how the volume $V[T, x^{\text{Fe}\downarrow}(T)]$ and the anomalous contribution to the LTEC $\alpha_a(T)$ vary as the temperature is raised. It is worth emphasizing that neither partial chemical order [24] nor static ionic displacement [33, 34, 35] has been explicitly taken into account at any stage.

Tests results for Fe_{0.72}Pt_{0.28}, Fe_{0.65}Ni_{0.35}, and Fe_{0.2}Ni_{0.8} have provided evidence that the methodology captures the essential physics of the Invar effect. This opens exciting opportunities for investigating the mechanism of the phenomenon, which, in principle,

can now be understood within the same framework as other intriguing observations [17].

We have decomposed the anomalous contribution to the LTEC α_a into two parts and studied each of them separately, for $\text{Fe}_{0.72}\text{Pt}_{0.28}$, $\text{Fe}_{0.65}\text{Ni}_{0.35}$, and $\text{Fe}_{0.2}\text{Ni}_{0.8}$. Our results support the following criterion: The Invar phenomenon occurs only when the thermal expansion arising from the temperature dependence of the fraction of Fe moments which point down $\alpha_{a,2}$ compensates for the thermal expansion associated with the anharmonicity of lattice vibrations α_n in a wide temperature interval.

Finally, based on the study of $\alpha_{a,2}$ and κ , we have predicted that only alloys with strong magnetostructural coupling at $T = 0\text{ K}$ can show the Invar effect. This work challenges the conventional picture of the Invar effect as resulting from peculiar magnetic behaviour.

Acknowledgments

The author thanks I. A. Abrikosov (Linköping), B. Alling (Linköping), C. A. Hooley (St Andrews, U.K.), A. E. Kissavos (Linköping), and J. Neugebauer (Düsseldorf) for fruitful discussions.

References

- [1] Guillaume C E 1897 *C.R. Acad. Sci.* **125** 235
- [2] Kussmann A and von Rittberg G 1950 *Z. Metallkd.* **41** 470
- [3] Oomi G and Mōri N 1981 *J. Phys. Soc. Jpn.* **50** 2924
- [4] Crangle J and Hallam G C 1963 *Proc. R. Soc. A* **272** 119
- [5] Sumiyama K, Shiga M, and Nakamura Y 1976 *J. Phys. Soc. Jpn.* **40** 996
- [6] Sumiyama K, Shiga M, Morioka M, and Nakamura Y 1979 *J. Phys. F: Met. Phys.* **9** 1665
- [7] Weiss R J 1963 *Proc. Phys. Soc.* **82** 281
- [8] Ullrich H and Hesse J 1984 *J. Magn. Magn. Mater.* **45** 315
- [9] Brown P J, Neumann K-U, and Ziebeck K R A 2001 *J. Phys.: Condens. Matter* **13** 1563
- [10] van Schilfgaarde M, Abrikosov I A and Johansson B 1999 *Nature* **400** 46
- [11] Dubrovinsky L, Dubrovinskaia N, Abrikosov I A, Vennström M, Westman F, Carlson S, van Schilfgaarde M, and Johansson B 2001 *Phys. Rev. Lett.* **86** 4851
- [12] Cowlam N and Wildes A R 2003 *J. Phys.: Condens. Matter* **15** 521
- [13] Kakehashi Y 1981 *J. Phys. Soc. Jpn.* **50** 2236
- [14] Khmelevskiy S, Turek I, and Mohn P 2003 *Phys. Rev. Lett.* **91** 037201
- [15] Staunton J, Gyorffy B L, Pindor A J, Stocks G M, and Winter H 1985 *J. Phys. F: Met. Phys.* **15** 1387
- [16] Johnson D D, Pinski F J, Staunton J B, Gyorffy B L, and Stocks G M 1990 *Physical Metallurgy of Controlled Expansion Invar-Type Alloys* ed Russel K C and Smith D F (Warrendale, PA: TMS)
- [17] Liot F 2014 Magnetization, magnetostriction, and their relationship in Invar $\text{Fe}_{1-x}\text{A}_x$ ($A = \text{Pt}, \text{Ni}$) *arXiv*
- [18] Liot F and Hooley C A 2012 Numerical Simulations of the Invar Effect in Fe-Ni, Fe-Pt, and Fe-Pd Ferromagnets *arXiv:1208.2850*
- [19] Tanji Y 1971 *J. Phys. Soc. Jpn.* **31** 1366
- [20] Abrikosov I A, Kissavos A E, Liot F, Alling B, Simak S I, Peil O, and Ruban A V 2007 *Phys. Rev. B* **76** 014434
- [21] Moruzzi V L, Janak J F, and Schwarz K 1988 *Phys. Rev. B* **37** 790

- [22] Moruzzi V L 1990 *Phys. Rev. B* **41** 6939
- [23] Herper H C, Hoffmann E, and Entel P 1999 *Phys. Rev. B* **60** 3839
- [24] Crisan V, Entel P, Ebert H, Akai H, Johnson D D, and Staunton J B 2002 *Phys. Rev. B* **66** 014416
- [25] Khmelevskiy S, Ruban A V, Kakehashi Y, Mohn P, and Johansson B 2005 *Phys. Rev. B* **72** 064510
- [26] Vitos L 2001 *Phys. Rev. B* **64** 014107
- [27] Wassermann E F 1990 *Ferromagnetic Materials* ed Buschow K H J and Wohlfahrt E P (Amsterdam: Elsevier)
- [28] Oomi G and Mōri N 1981 *J. Phys. Soc. Jpn.* **50** 2917
- [29] Mañosa L, Saunders G A, Radhi H, Kawald U, Pelzl J, and Bach H 1991 *J. Phys.: Condens. Matter* **3** 2273
- [30] Decremps F and Nataf L 2004 *Phys. Rev. Lett.* **92** 157204
- [31] Rellinghaus B, Kästner J, Schneider T, Wassermann E F, and Mohn P 1995 *Phys. Rev. B* **51** 2983
- [32] Hayase M, Shiga M, and Nakamura Y 1973 *J. Phys. Soc. Jpn.* **34** 925
- [33] Liot F, Simak S I, and Abrikosov I A 2006 *J. Appl. Phys.* **99** 08P906
- [34] Liot F and Abrikosov I A 2009 *Phys. Rev. B* **79** 014202
- [35] Liot F 2009 *Thermal Expansion and Local Environment Effects in Ferromagnetic Iron-Based Alloys: A Theoretical Study* PhD dissertation (Linköping: Linköping University Electronic Press)